Supplemental Table 1

cDNA primers

Mus GAPDH	5’-CCA GCC TCG TCC CGT AGA CA-3’
	5'- GCC TCA CCC CAT TTG ATG TTA GTG -3'
Mus CCSP	5’- ACA TCA CCC CAC ATC TAC AGA CAC CAA -3’
	5’- TGA GGA GGG CCT CAA GGA CTT GAA -3’
MDM2	5’- TGG CGT GCC AAG CTT CTC TGT-3’
	5’- ACC TGA GTC CGA TGA TTC CTG CT -3’
Mus cyclin D2	5’-AAA TGG GGG CAG ATG GAG A -3’
	5’-GGC AAA GGA GGA AGG CGT AT -3’
Mus Hes1	5'- TGA AGG ATT CCA AAA ATA AAA TTC TCT GGG -3'
	5'- CGC CTC TTC TCC ATG ATA GGC TTT GAT GA -3'

Supplemental Table 2

Genotyping primers

pTREtightMDM2	5'- CTG TGA GTG AGA ACA GGT GTC AC -3'
	5'- GGC TAT AAT CTT CTG AGT CGA GAG -3'
p53 +/-	5'- AGC GTG GTG GTA CCT TAT GAG C-3'
	5'- GGA TGG TGG TAT ACT CAG AGC C-3'
	5'- GCT ATC AGG ACA TAG CGT TGG C-3'
Mdm2 +/-	5'- TGT GGC TGG AGC ATG GGT ATT G-3'
	5'- ATC TGA GAG CTC GTG CCC TTC G-3'
	5'- GGC GGA AAG AAC CAG CTG GGG C-3'

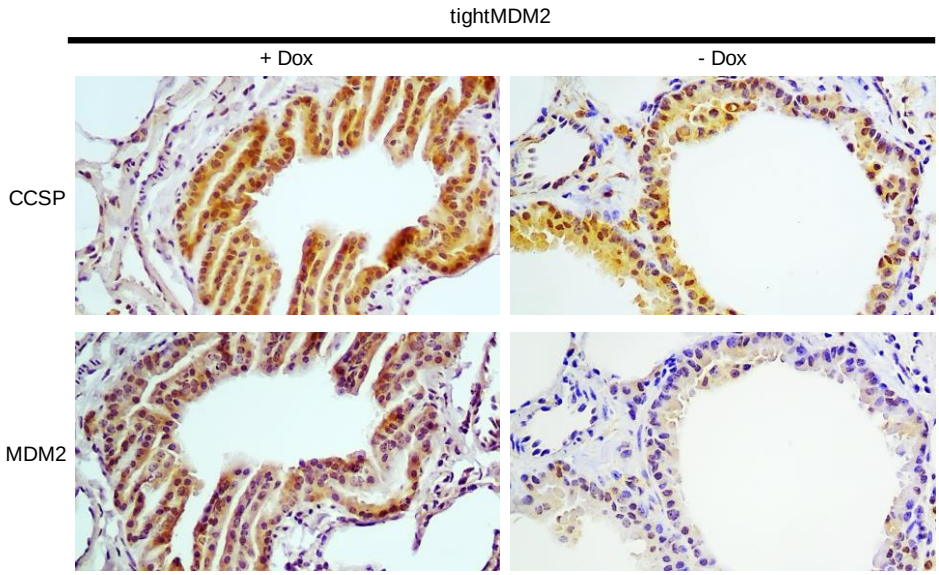

Supplemental Figure S1: Induction of MDM2 expression in CCSP-expressing lung Club cells. Immunostaining of serial FFPE lung tissue sections from Dox-treated (Dox+) or sucrose-treated (Dox-) tightMDM2 mice show CCSP (brown) and MDM2 (brown) expression in lung Club cells around respiratory bronchiole. Representative images (Magnification: 20X) are shown. Experiments were repeated in 3 mice.

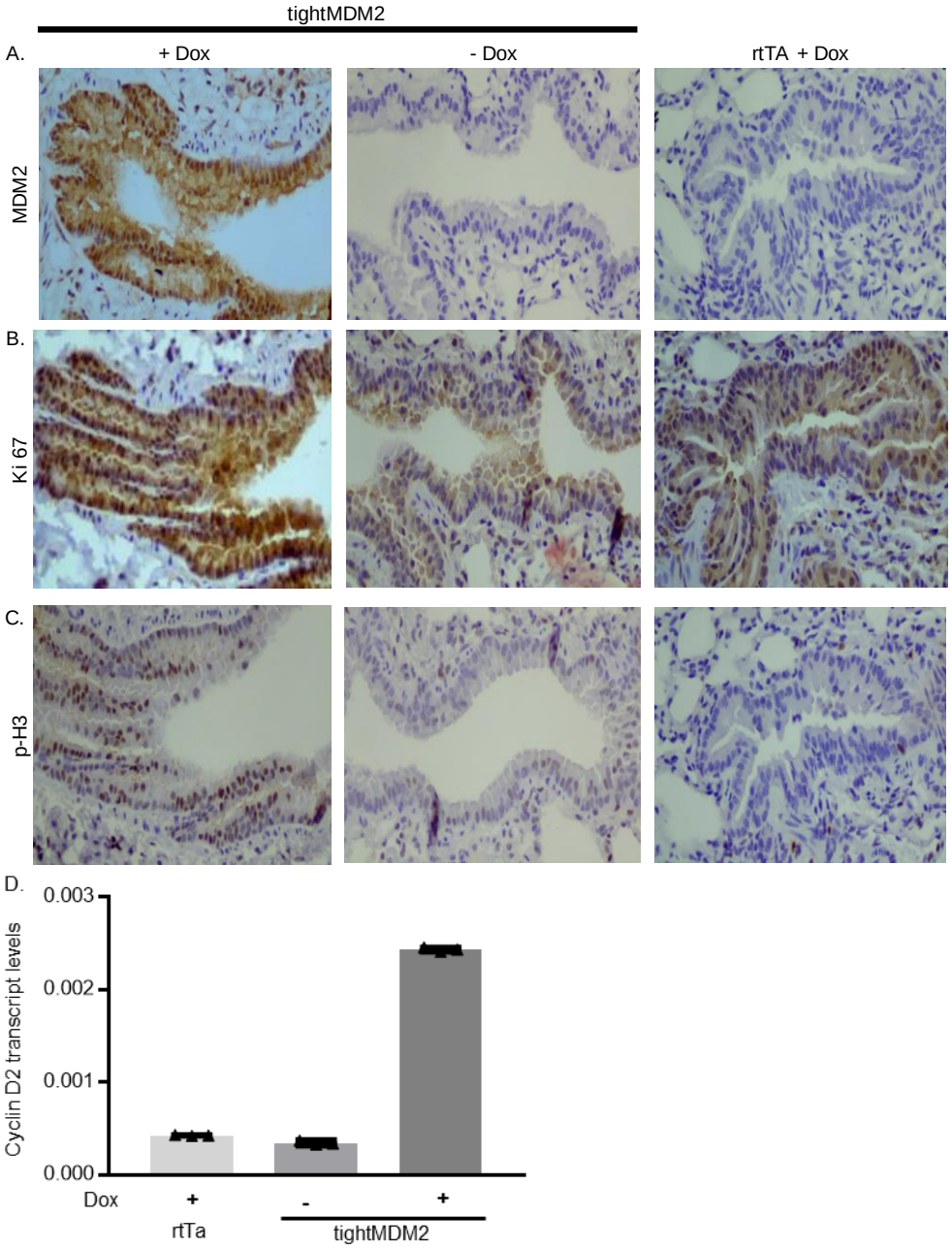

Supplemental Figure S2: **Induction of MDM2 expression in lung Club cells increases expression of interphase markers but does not induce BrdU incorporation**. Immunostaining of serial FFPE lung tissue sections from Dox-treated (Dox+) or sucrose-treated (Dox-) tightMDM2 mice and Dox-treated rtTA mice show (**A**) MDM2 (brown), (**B**) Ki67 (brown), and (**C**) p-H3 (brown) expression in lung Club cells around respiratory bronchiole. Representative images (Magnification: 20X) are shown. (**D**) Cyclin D2 transcript levels from lung tissues of Dox-treated control rtTA and Dox-treated or -untreated tightMDM2 mice determined by QRTPCR performed in triplicate. Transcript levels were normalized by GAPDH expression and are plotted as mean ± SD. All experiments were repeated in at least 3 mice per treatment. Representative data shown.

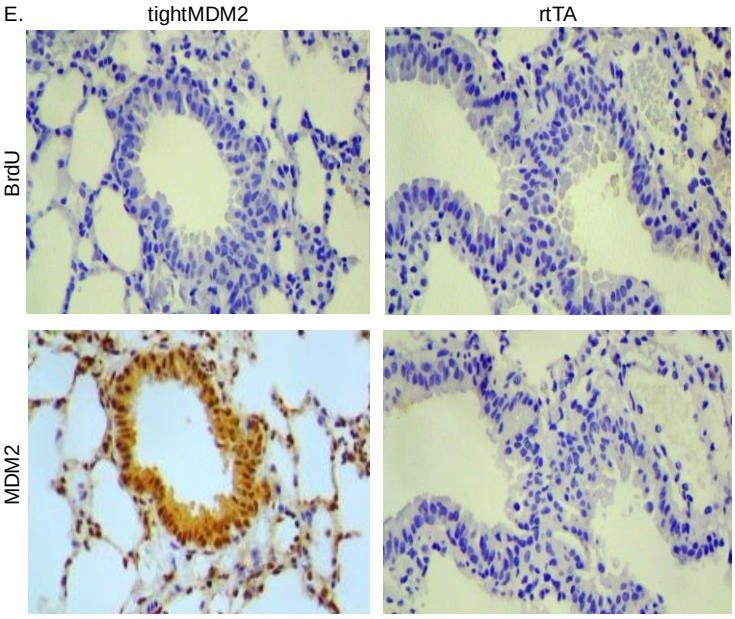

Supplemental Figure S2 (contd.): (**E**) Immunostaining of BrdU and MDM2 (brown) in serial lung tissue sections from Dox-treated tightMDM2 and rtTA mice after BrdU delivery. Representative images (Magnification: 20X) are shown. All experiments were repeated in at least 3 mice.

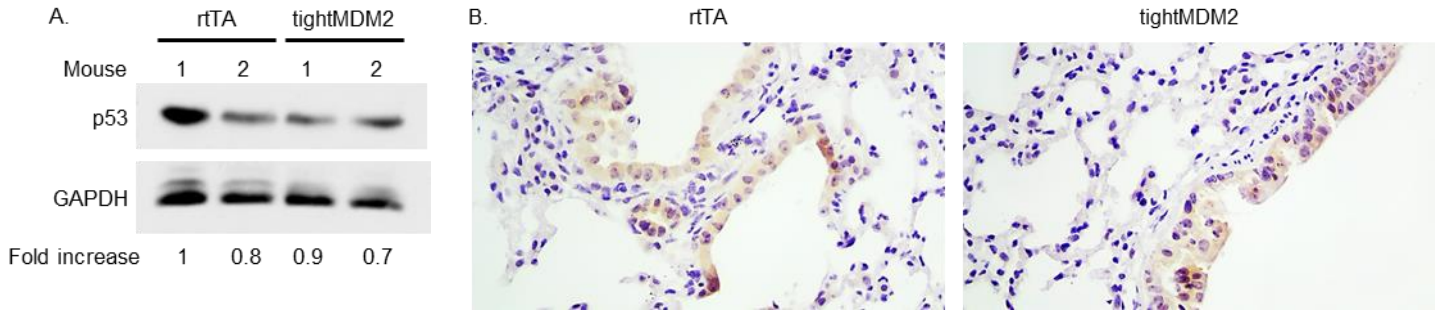

Supplemental Figure S3: **Consequent to naphthalene injury, Dox-induced MDM2 expression does not significantly alter p53 levels, and loss of WT p53 does not escalate DNA replication, CCSP/SPC dual positive bronchiolar cell proliferation and epithelial repair in lung bronchioles**. (**A**) Immunoblot analysis of p53 and GAPDH (loading control). Fold increase of p53 expression was determined by densitometry and is shown at the bottom of the immunoblot (**B**) Immunostaining of FFPE lung tissue sections from Dox-treated (Dox+) tightMDM2 and Dox+ rtTA mice show p53 levels in lung bronchiolar cells. Representative images (Magnification: 20X) are shown. All experiments were repeated in at least 3 mice.

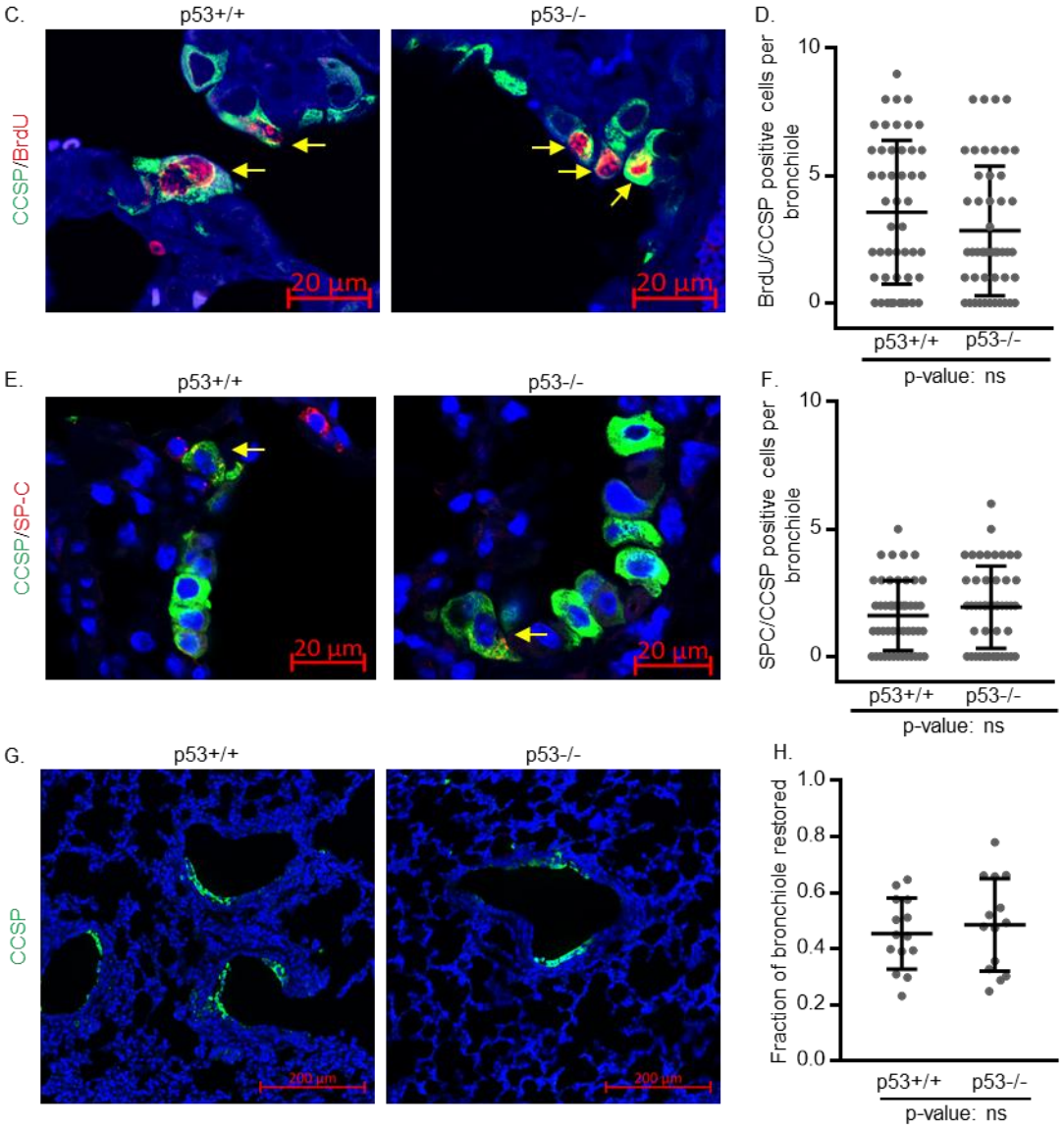

Supplemental Figure S3 (contd.): FFPE lung sections of indicated mouse constructs were analyzed by immunostaining after naphthalene injury and BrdU delivery Representative images (Magnification: 40X) showing (**C**) BrdU incorporation (red) in CCSP (green) expressing cells in lung bronchioles, (**D**) Dot plot showing frequency of BrdU incorporating CCSP positive cells. (**E**) Representative images (Magnification: 40X) showing CCSP (green) and SPC (red) co-expressing progenitor cells (arrows) in lung bronchioles, (**F**) Dot plot showing frequency of CCSP and SPC co-expressing cells in lung bronchioles. Data for each treatment were collected from three mice, 16 bronchioles from each mouse and plotted as mean ± SD (n = 48). (**G**) Representative images (Magnification: 10X) showing restoration of epithelial layer with CCSP expressing cells in lung bronchioles, (**H**) Dot plot showing fraction of bronchioles restored. Data for each treatment was collected from three mice, 5 bronchioles per mouse and plotted as mean ± SD (n = 15). In all graphs, p-values calculated using Student's *t* test are indicated.

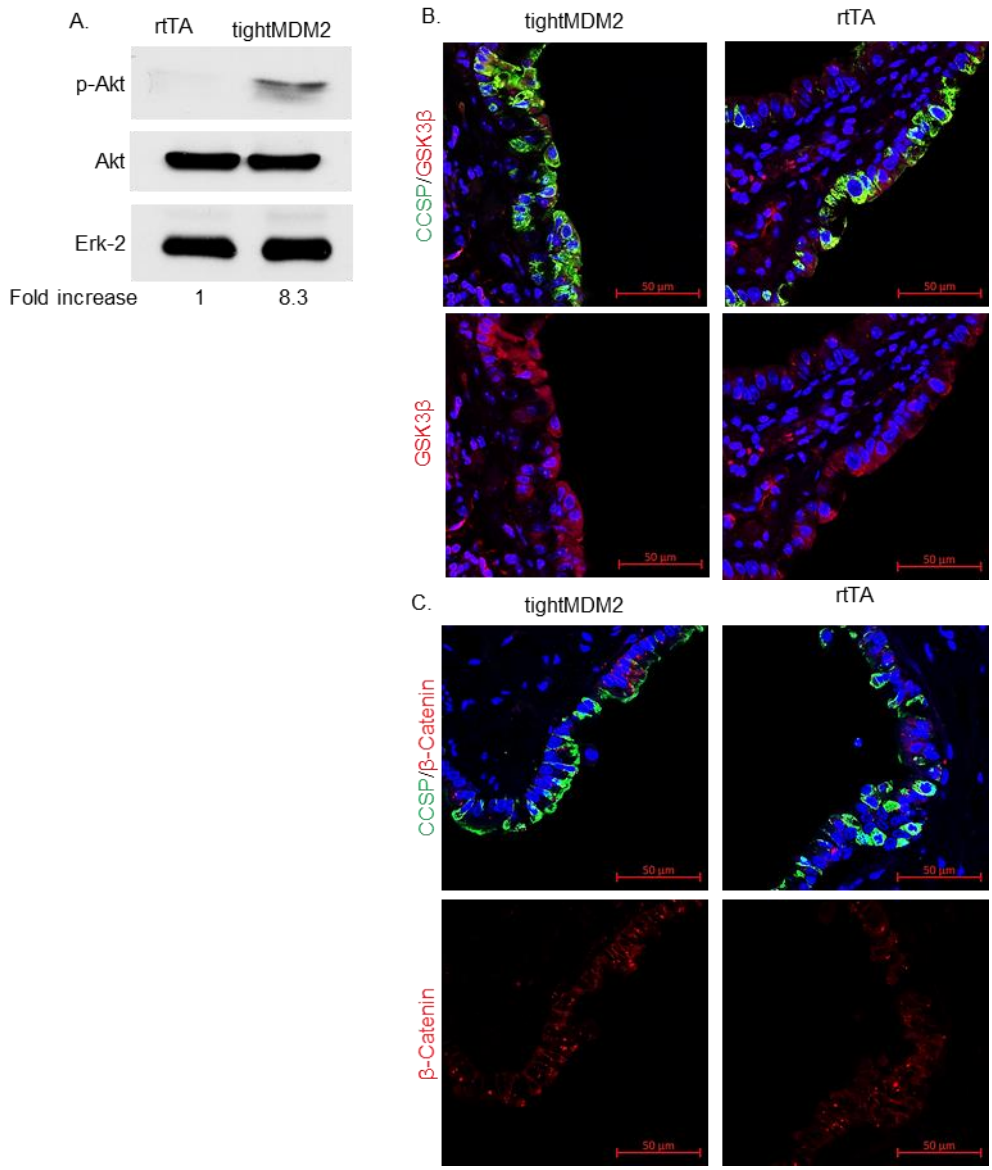

Supplemental Figure S4: **MDM2 activates Akt phosphorylation but does not increase unphosphorylated GSK3β or β-Catenin levels after naphthalene treatment for 72 hours.** (**A**) Immunoblot analysis of naphthalene-treated lung tissue extracts for Akt phosphorylation at Ser 473. Fold increase in p-Akt levels was determined by densitometry and is shown at the bottom of the immunoblot comparing band intensities for a third set of mice, while data for two sets of mice are shown in Figure 3 (main text). Immunostaining of FFPE tissue sections (**B**) GSK3β (red) and (**C**) β-Catenin (red) in CCSP expressing (green) cells. Representative images (Magnification: 40X) are shown. Data for each treatment was collected from three mice.

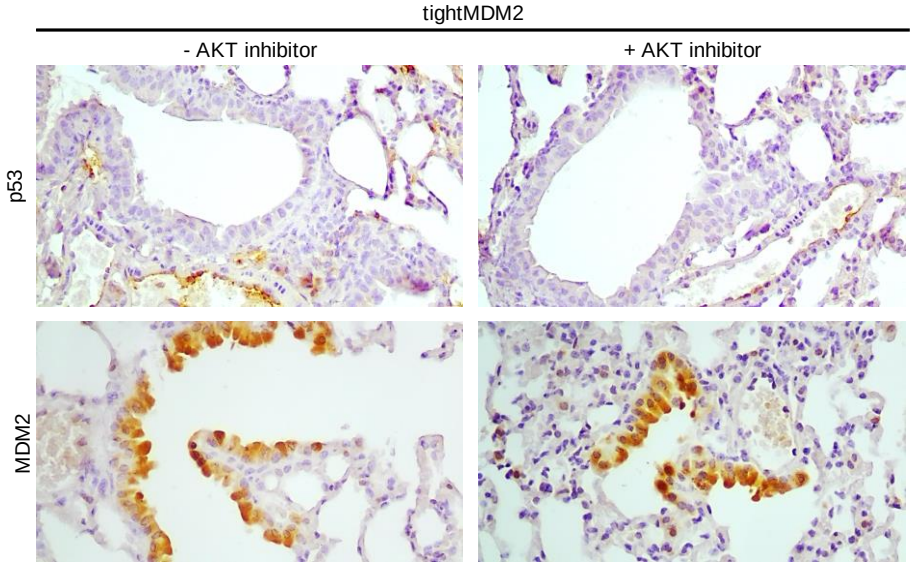

Supplemental Figure S5: **AKT inhibitor MK-2206 does not significantly alter p53 levels in lung Club cells upon Dox-induced MDM2 expression and naphthalene treatment**. Immunostaining of FFPE lung tissue sections from Dox-treated (Dox+) tightMDM2 mice 72 hours after naphthalene-treatment in the presence or absence of MK-2206 for MDM2 (brown) and p53 (brown) expression in lung bronchiolar cells. Representative images (Magnification: 20X) are shown. All experiments were repeated in at least 3 mice.

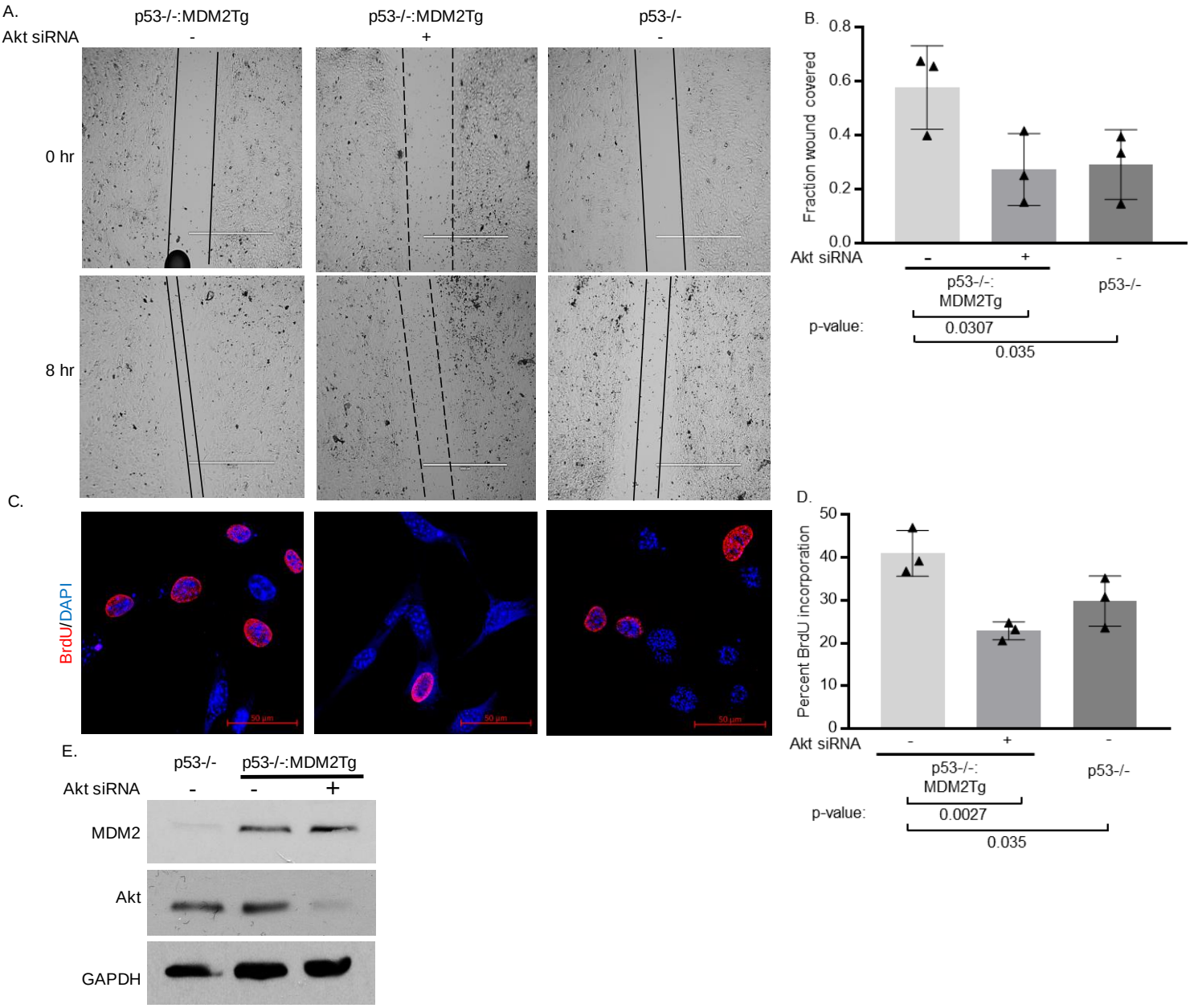

Supplemental Figure S6: Depletion of Akt in early passage lung cells inhibits MDM2-induced wound healing and DNA replication in the absence of p53. Akt siRNA was introduced into early passage primary lung cells isolated from p53-null:MDM2 transgenic (p53-/-:MDM2Tg) mice. (**A**) Wound areas in monolayer cell culture in the presence or absence of Akt siRNA is shown by straight lines (solid or broken) at 0 and 8 hours after Akt siRNA delivery. p53-/- lung cells were used as controls. (**B**) Fraction of wound area covered in 8 hours are shown. (**C**) Confocal images (Magnification 20X) show frequency of BrdU incorporating (red) cells. (**D**) Percent of BrdU incorporating (red) cells in the absence or presence of Akt siRNA were counted and are shown. Representative images (Magnification: 40X) are shown. (**E**) Immunoblot analysis to show MDM2 expression and depletion of Akt by Akt siRNA. All graphs are presented as mean ± SD. p-value calculated using Student's *t* test. All experiments were done in triplicates.

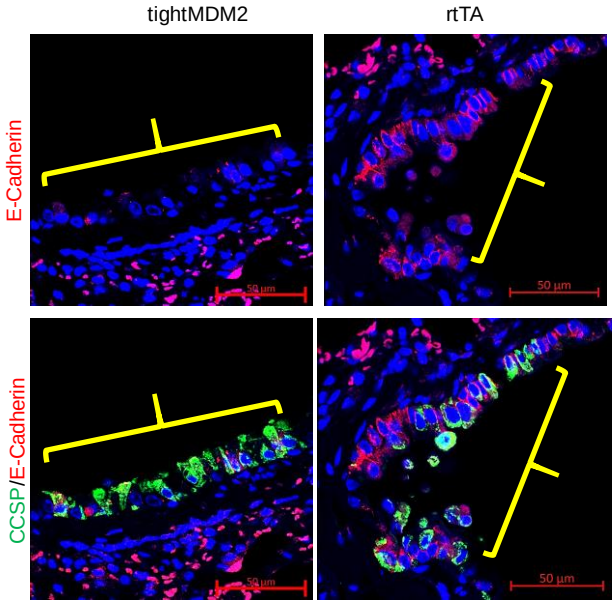

Supplemental Figure S7: MDM2 reduces expression of EMT marker E-Cadherin consequent to naphthalene-induced lung injury. Representative images (Magnification: 40X) of FFPE lung sections after immunostaining of E-Cadherin (red) in CCSP expressing (green) cells of lung bronchiole (yellow brackets). Representative images (Magnification: 20X) are shown. All experiments were repeated in at least 3 mice.

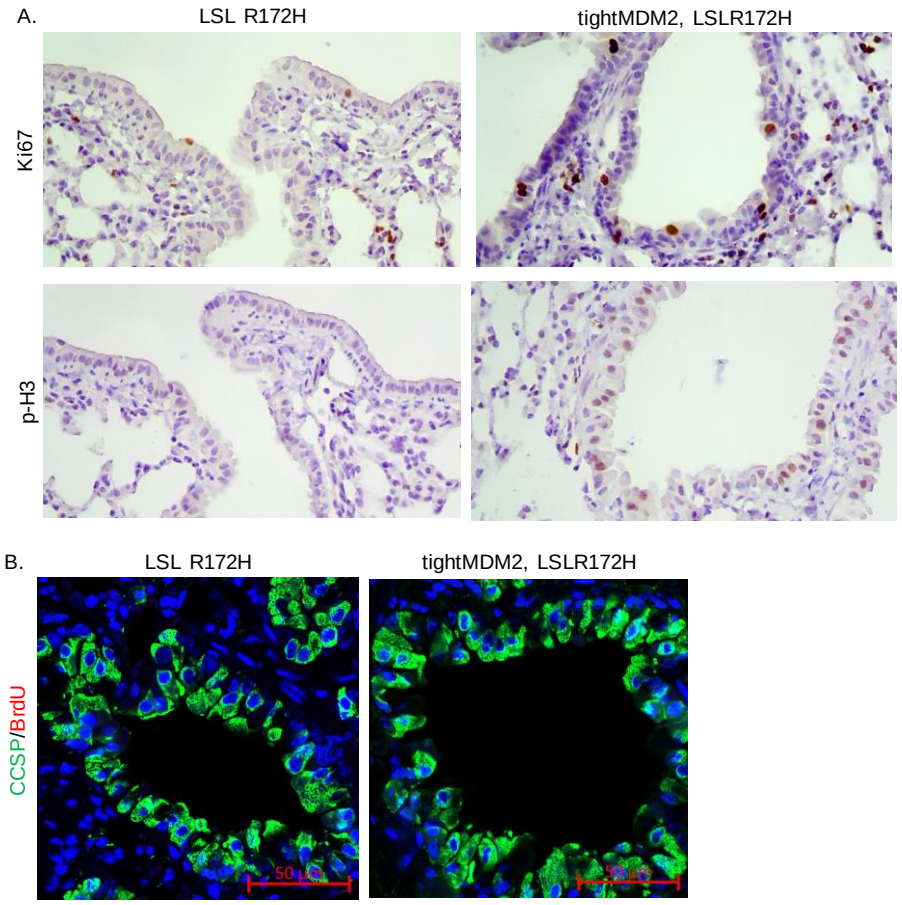

Supplemental Figure S8: Induction of MDM2 and p53-R172H co-expression in lung Club cells (Figure 7A) increases expression of proliferation markers but does not induce BrdU incorporation. (**A**) Immunostaining of serial FFPE lung tissue sections from Dox-treated LSL R172H and LSL R172H, tightMDM2 mice show (A) Ki67 (brown), and p-H3 (brown) expression in lung Club cells around respiratory bronchiole (Magnification: 20X), (**B**) but not BrdU-incorporating cells after BrdU delivery (Magnification: 40X). Representative images are shown. All experiments were repeated in at least 3 mice.

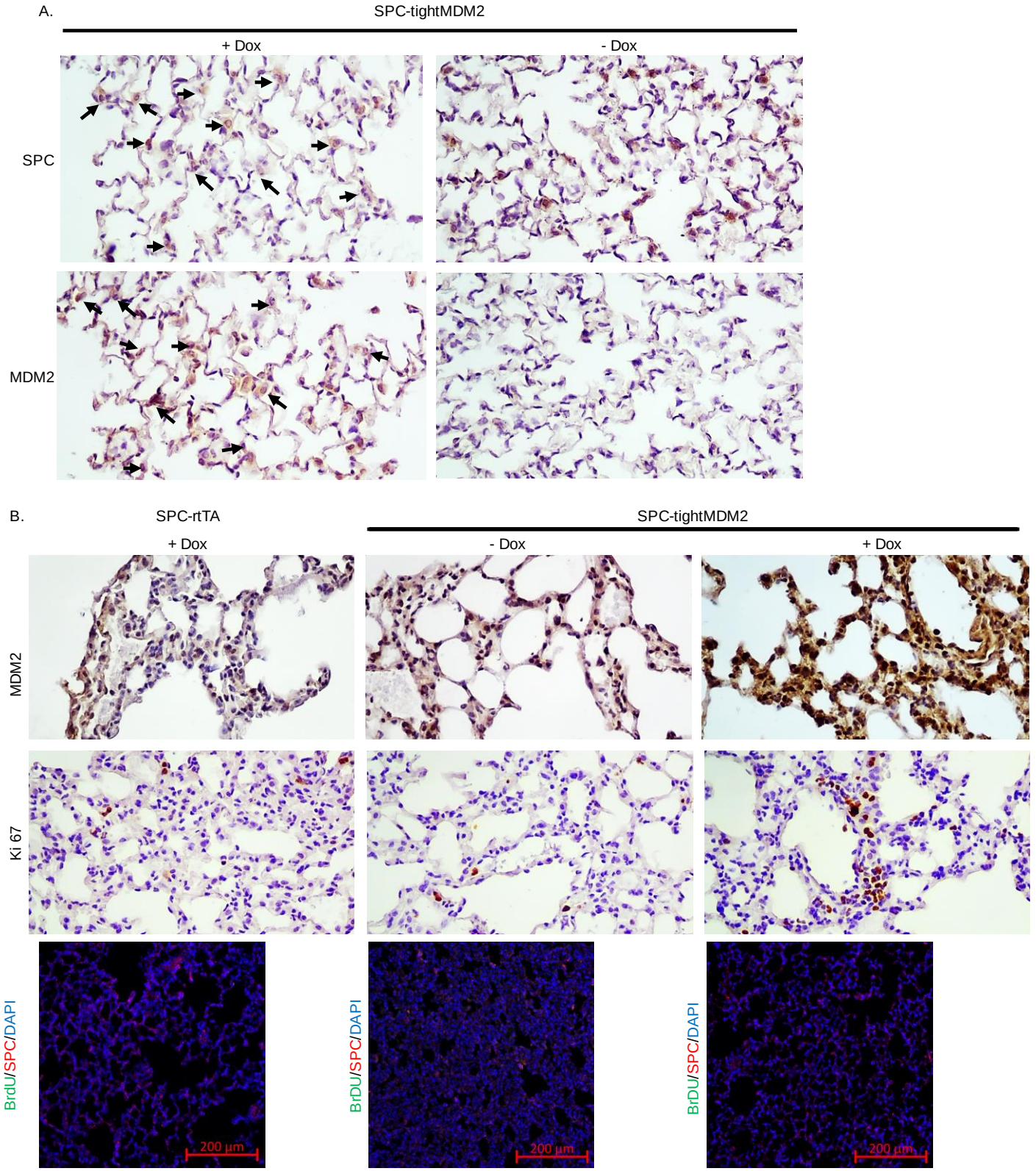

Supplemental Figure 9: **Induction of MDM2 expression in lung alveolar cells increases expression of proliferation markers but does not induce BrdU incorporation in cells.** Immunostaining of serial lung tissue sections from Dox-treated or untreated SPC-tightMDM2 or Dox-treated SPC-rtTA or mice show (**A**) MDM2 (brown) in SPC positive (brown) cells (arrows), (**B**) MDM2 (brown) and Ki67 (brown) expression (Magnification: 20X), but not BrdU-incorporating cells after BrdU delivery (Magnification: 10X)

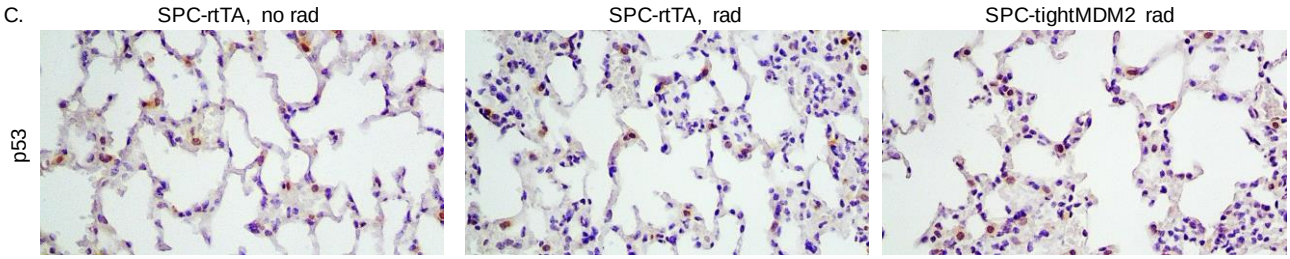

Supplemental Figure 9 (contd): (**C**) Images (Magnification: 20X) show immunostaining for p53 expression (brown) in FFPE lung tissue sections from Dox-treated SPC-tightMDM2 or SPC-rtTA mice 3 months after radiation (rad) or no radiation (no rad). Representative images are shown. All experiments were repeated in at least 3 mice.

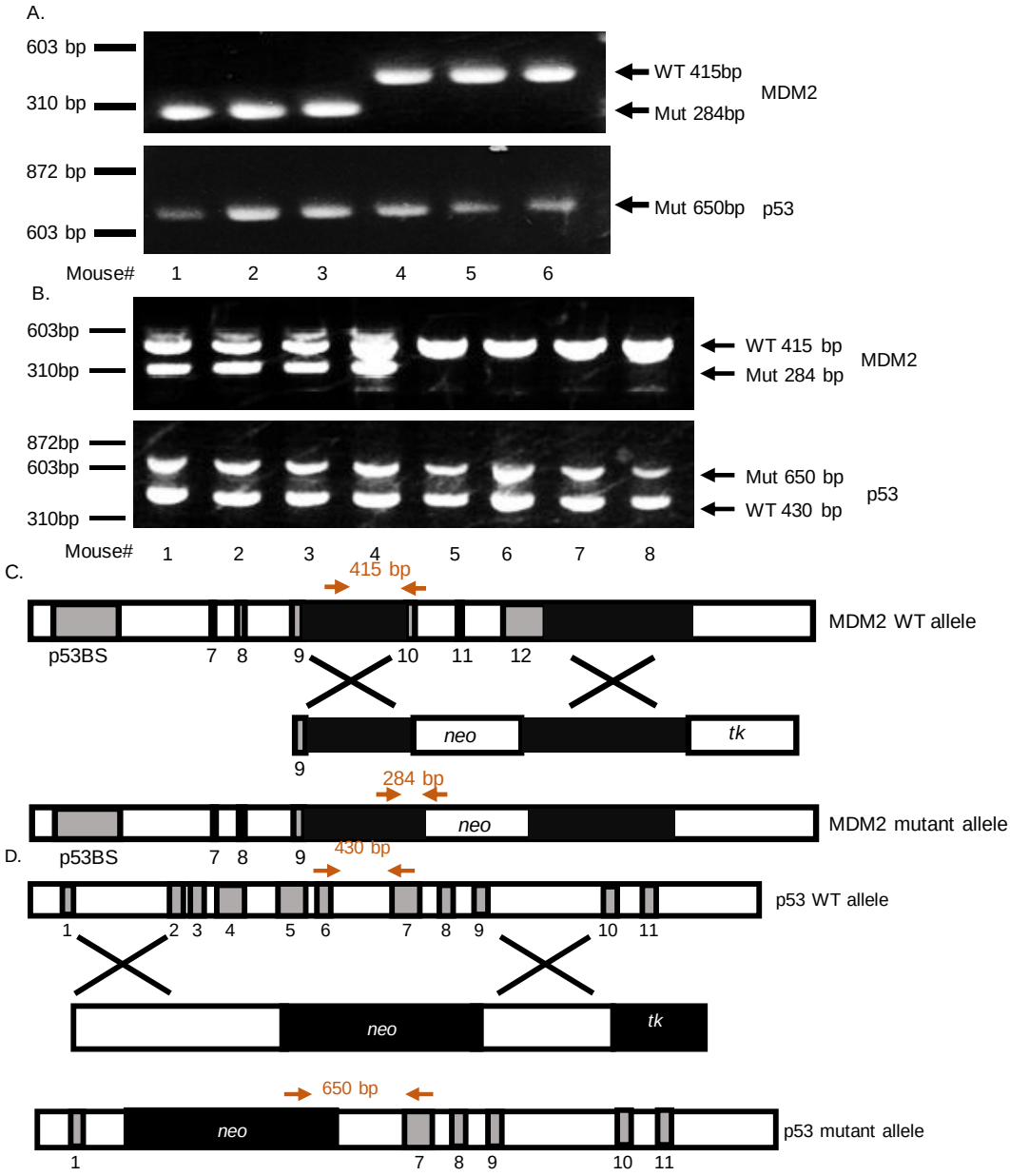

Supplemental Figure S10: **Genotyping of** (**A**) **p53-/- mdm2+/+ and p53-/-:mdm2-/-; and** (**B**) **p53+/-:mdm2+/+ and p53+/-:mdm2+/- mice**. PCR products of DNA prepared from clipped tail using primers shown in (**C**) and (**D**) were resolved by agarose gel electrophoresis. Expected fragment sizes (shown in red) for MDM2 (C) and p53 (D) WT and mutant allele are shown by schematics. Primer sequences have been described in Supplemental Table 2

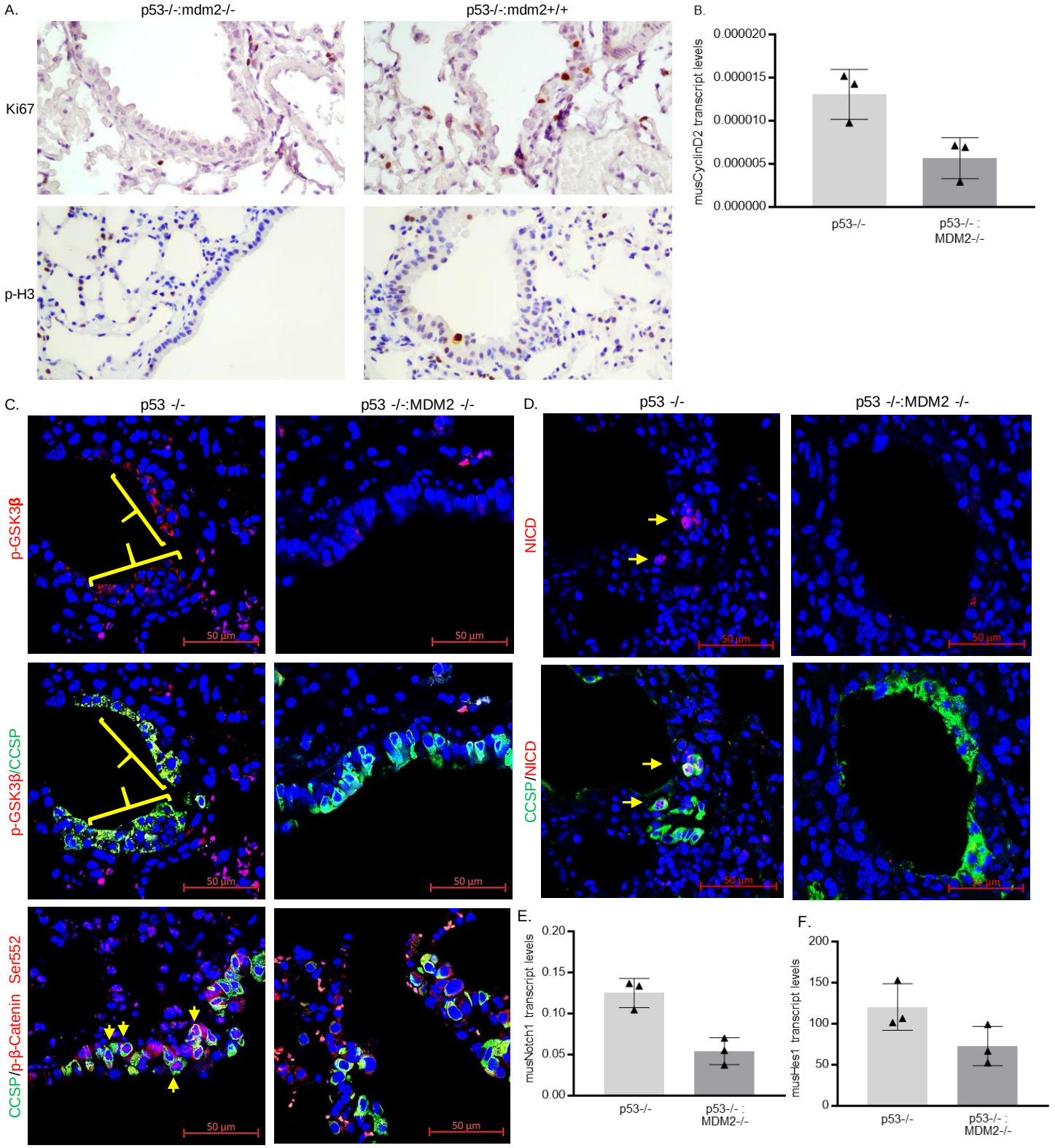

Supplemental Figure S11: Endogenous MDM2 activates the Akt signaling pathway consequent to naphthalene injury. Lung FFPE tissue sections or cDNA from p53-/- or p53-/-:MDM2-/- mice harvested 48 hours after naphthalene treatment show **(A)** reduced frequency of Ki67 and p-H3 positive cells **(B)** reduced expression of Cyclin D2 transcripts, drastic reduction in **(C)** the Akt target GSK3β phosphorylation at Ser 9 (red), **(D)** NICD levels and its nuclear translocation in CCSP expressing (green) cells (brackets or arrows), and expression of (**E**) Notch1 and (**F**) Hes1 transcripts**.** Representative images (Magnification for A is 20X, C-D is

40X) are shown. Representative plots from a set of mice plotted as mean ± SD. Data for each treatment was repeated in three sets of mice.